TAO, Vol. 9, No. 3, 317-328, September 1998

Preliminary Crustal Structures Across Central Taiwan From Modeling of the Onshore-Offshore Wide-Angle Seismic Data

R. C. Shih[1], C. H. Lin[2], H. L. Lai[1], Y. H. Yeh[2], B. S. Huang[2], and H. Y. Yen[3]

(Manuscript received 22 January 1998, in final form 31 August 1998)

ABSTRACT

Wide-angle reflection and refraction data are used to illustrate the crustal structures in the central Taiwan area, across the Taiwan Orogen and in the westernmost part of the Ryukyu subduction system. The preliminary structures were derived by modeling the data set collected using onshore seismic recording instruments along the central cross-island highway in 1995. Seismic signals were generated by the powerful airgun arrays of the R/V Ewing in the seas east of Taiwan. For the shallow structures, results from the forward modeling of the Pg phases show that strong lateral variations of P-wave velocities in the upper crust were obtained. Velocities at the uppermost crust have a wide range from 3.0 km/sec to 5.2 km/sec, and increase from 5.8 km/sec to 6.8 km/sec at the bottom of the upper crust. The thickness of the upper crust increases from 22 km beneath the Western Central Range to 25 km beneath the Hsincheng Ridge, and it then dramatically decrease to only 10 km beneath the Hoping and Nanao basins. For the deep crust structures, similar pattern of thickness variations, from 12 km to 20 km, was obtained. Velocities at the lower crust range from 6.4 - 6.7 km/sec at its top to 7.2 - 7.3 km/sec at its bottom. In summary, the crustal thickness beneath the island could be over 40 km, but only about 25 km beneath the westernmost part of the Ryukyu forearc region. The thickest crust is not right beneath the highest mountains on the island but with an offset of about 40 km toward the east. The result indicates that Taiwan has still not yet reached to its isostatic equilibrium yet.

(Key words: Wide-angle seismic profiling, Deep crustal structures, Central Taiwan)

1. INTRODUCTION

The island of Taiwan is located at a complex part of the convergent boundary between the Eurasian and Philippine Sea plates. East of the island, the Philippine Sea plate has subducted

[1]Inst. of Seismology, National Chung Cheng University, Chiayi, Taiwan, ROC
[2]Inst. of Earth Sciences, Academia Sinica, Taipei, Taiwan, ROC
[3]Inst. of Geophysics, National Central University, Chungli, Taiwan, ROC

northward beneath the Eurasian plate along the Ryukyu trench. South of the island, the Eurasian plate underthrusts the Philippine Sea plate along the Manila trench (Biq, 1972; Bowin *et al.*, 1978; Tsai, 1978; Ho, 1982; Angelier and Barrier, 1986; Pelletier and Stephan, 1986; Roecker *et al.*, 1987). Taiwan is an artifact of an ongoing collision between the Eurasian plate and Luzon volcanic arc at the northwestern edge of the Philippine Sea plate. The collision has been propagating from north to south due to an oblique orientation of the Luzon arc with respect to the Eurasian plate generating the Taiwan Orogen. However, our understanding of the Taiwan Orogen is still very limited, because of the absence of key information such as the geometry of the crust near the plate boundary.

Although the crustal structures of Taiwan have been investigated by a number of scientists (Yeh and Tsai, 1980; Rau and Wu, 1995; Chen, 1996; Lin, 1996), there have been some strong disagreements between them. The crustal thickness has been interpreted within a wide range, from 33 km to 65 km in the Taiwan area. The crustal thickness in Taiwan was first studied by Yeh and Tsai (1981), who obtained a one-dimensional Moho depth of 36 km, based on the inversion results of a few local earthquakes recorded at several stations on the TTSN (Taiwan Tele-Seismic Network) in central Taiwan. Since then, their results have been used as a velocity model for routinely locating earthquakes in Taiwan, and commonly employed as a standard crustal structure for further studies. Their results were more or less confirmed by the investigation of gravity data, which showed a crustal thickness of about 33-37 km (Chen, 1996). However, the above results have been challenged by some more recent seismological studies. For example, Rau and Wu (1995) indicated that according to seismic tomography, the crustal thickness could be over 65 km beneath central Taiwan. Furthermore, Lin (1996) noted that the maximum crustal thickness in Taiwan could be up to 45-50 km, based on the observations of the differences between the first P-wave arrivals at two nearby stations. In short, the large differences in the crustal thickness range are attributed to the absence of more reliable data.

In this paper, onshore/offshore wide-angle seismic data are used to illustrate a two-dimensional cross-section of the crustal structure across the central Taiwan area. The wide-angle seismic data were collected by the seismic recording instruments deployed along the central cross-island highway. Source signals were generated by the powerful airgun arrays of the R/V Maurice Ewing offshore from eastern Taiwan. Detailed descriptions of the onshore/offshore experiment are presented in the paper by Yeh *et al.* (1998; this issue). Consequently, the results of modeling will show the characteristics of the upper crust and will also provide strong constraints on the deep crustal structures. The results of this research should improve the understanding of the transitional characteristics between the Taiwan Orogen and the westernmost part of the Ryukyu subduction system.

2. GEOLOGICAL SETTING

Geologic units on the central part of Taiwan include, from west to east, the Coastal Plain, the Western Foothill, the Western Central Range and the Eastern Central Range. These units, roughly striking NNE-SSW, are often bounded by faults or other discontinuities (Ho, 1982). All of them belong to the continental margin of the Eurasian plate. Metamorphic rocks are

largely exposed at the surface of the Eastern and Western Central Ranges, which constitute a major part of the Taiwan Orogeny. Indurated to metamorphosed sandstones predominate in the Western Central Range, while schists and metamorphosed limestones make up the Eastern Central Range. The Western Foothills are composed of Oligocene to Pleistocene clastic sediments. These sediments have been stacked up by a combination of northwest-vergent folds and low-angle thrust faults dipping to the southeast. To the west, the Coastal Plain is composed of Quaternary alluvial deposits derived from the Central Range and the Western Foothills.

Offshore from eastern central Taiwan, is the profile under study, which cuts through the Hsincheng Ridge and several basins (Figure 1). The Hsincheng Ridge, a bathymetric high, is located just offshore from the Eastern Central Range. Farther east, there are several forearc basins that are parts of a convergent margin structure along the Ryukyu subduction system (Liu *et al.*, 1997). The forearc basins from west to east include the Hoping Basin, the Nanao Basin and the East Nanao Basin. The shallow structures of these basins are revealed by the seismic profile EW9609-14 of the TAICRUST project (Liu *et al.*, 1997). The basins, which lie on top of an undulating arc basement, are separated by basement highs. The depths of these basins become shallower westward. Seismic reflection characteristics of the forearc basin sediments indicate that they mainly consist of turbidite sequences derived from the Taiwan mountain belt.

3. SEISMIC DATA AND PHASE IDENTIFICATION

The wide-angle reflection and refraction seismic data used in this study were collected in August and September of 1995 during the TAICRUST experiment. Onshore, 35 seismic recording instruments were deployed along the central cross-island highway with an average spacing of 3.5 km. The R/V Maurice Ewing, shooting offshore from eastern Taiwan with a 20-airgun array (8420 in^3 total volume) provided the seismic sources.

This profile is approximately perpendicular to the strike of the main structures of Taiwan (Figure 1). From west to east, it cut through different geological units on the surface, including the Coastal Plain, the Western Foothills, the Western Central Range and the Eastern Central Range. The profile extends eastward offshore from the coast through the Hoping Basin, the Nanao Basin and the East Nanao Basin. These basins are forearc basins belonging to the westernmost part of the convergent margin along the Ryukyu subduction system (Liu *et al.*, 1997).

During data acquisition, airguns from the R/V Maurice Ewing were fired every 40 seconds. Seismic signals were recorded using a 4.5 Hz three-component velocity-type seismometer at each station, and sampled every 10 ms. The 35 onshore seismic stations were deployed to form a linear array of 116 km in length. A total of 1,256 airgun shots was generated offshore, over a distance of about 133 km, from just east of the coastline to the eastern end of the profile. The shot times were synchronized at all stations using the GPS.

The recorded seismic data were processed by a number of processing strategies. Firstly, the continuously recorded seismic data were sorted into a common-receiver gather of 1256 traces, 40 seconds in length. Secondly, the spiky anomalies were removed, and a band-pass

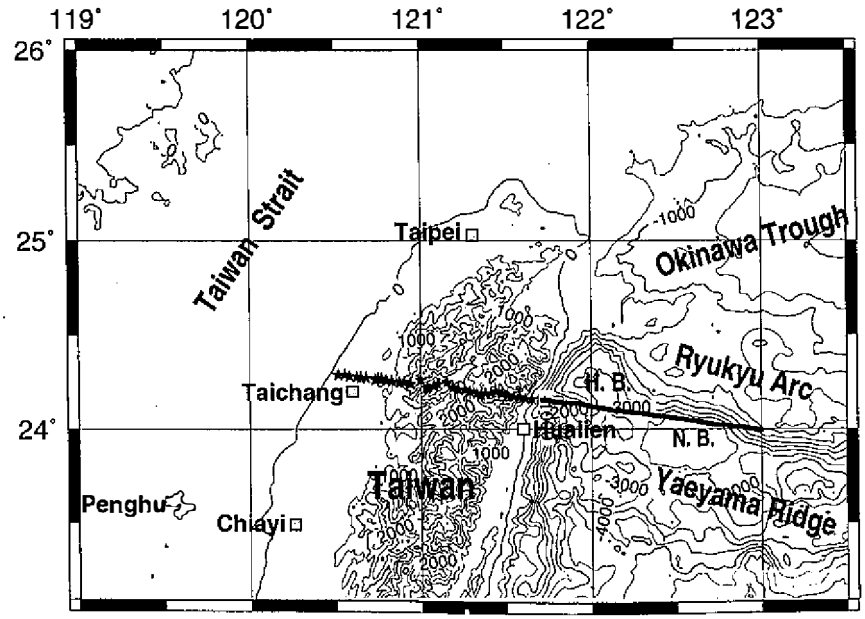

Fig. 1. Locations of onshore seismic stations (star symbols) and offshore airgun shots (thick line) across Central Taiwan. Topographic relief and bathymetry are also shown. Locations of Hoping and Nanao basins are marked by H.B. and N.B., respectively.

filtering of 4 - 10 Hz was applied to all traces. After that, a spherical divergent correction was applied to compensate the seismic energy, and the energy between traces was balanced. Finally, we mixed the two adjacent traces and applied spiking deconvolution to improve the signal to noise ratio. After the above processing steps, we displayed the common-receiver gathers with automatic gain control (AGC) to enhance the interested targets.

In this study, only seismic events that could be clearly identified were used for modeling the crustal structures. Figure 2 shows the common-receiver gather at station 29 in the Eastern Central Range, in which we may see clear coherent phases including the direct phases (Pg), the reflected phases (PcP) and the refracted phases (Pc) within the crust, as well as the reflected phases (PmP) from the uppermost mantle. Most of these phases were identified directly according to their characteristics including amplitude and apparent velocity.

In addition, the most important criteria for recognizing the coherent phase was done by using modeling of the travel times of coherent phases. The forward modeling technique is to compare the arrivals of each phase and the slope of whole group phases with the calculated results based on a given model. Figure 3 shows an example of ray diagrams of different phases and their arrival times as recorded at one station. The arrivals of all phases are plotted with distances versus 8 km/sec reduced travel times. The Pg phases arrive between 4 and 6 seconds at the reduced travel time. They penetrated only to the uppermost crust and traveled at smaller offsets of about 50-60 km between the station and shots. The Pc phases, which are the re-

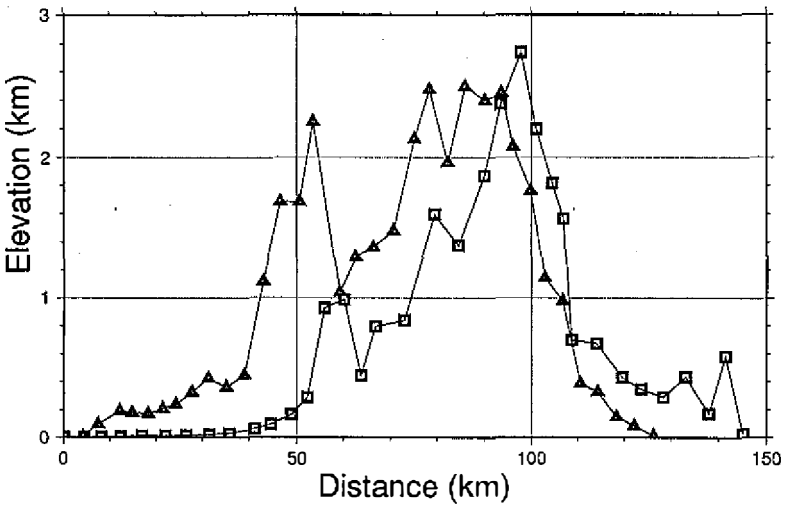

Fig. 2. One of the common-receiver gathers (at station 29) showing clear phases of Pg, Pc, Pn, and PmP.

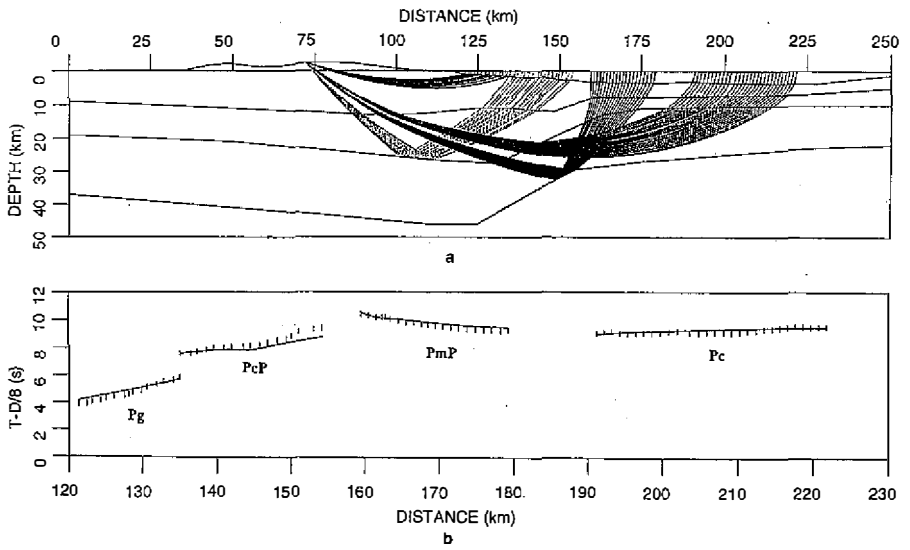

Fig. 3. Synthetic ray diagrams and their arrivals from data received at one station.

fracted arrivals from the lower crust, traveled larger distances of 120-150 km, arriving at reduced times of around 9 seconds. The PcP and PmP phases, which are the seismic signals reflected from the mid-crust and the Moho-discontinuities, respectively, arrive at reduced times of 8-11 seconds. Furthermore, it is noted that the slopes of the PcP and PmP phases are quite different. The positive slope of the PcP phases indicates that the apparent velocity is less than

8 km/sec, while the negative slope of the PmP phases shows that the apparent velocity is greater than the reduced (*i.e.* 8 km/sec). This phenomenon is largely attributed to the different dipping directions of the interfaces between them.

4. FORWARD MODELING

In this study, we employed the forward modeling algorithm developed by Zelt and Smith (1992) to construct the model of the crustal structures. The parameterization used here is a layered, variable-block-size representation of a two-dimensional isotropic velocity structure. Each layer is divided laterally into trapezoidal blocks by vertical boundaries wherever there was an upper or lower layer boundary node at a velocity point. Although velocity discontinuities may exist across layer boundaries, the velocity is laterally continuous within layers across the vertical boundaries. A layer boundary can represent an interface without an associated velocity discontinuity by applying the velocity from the base of the upper layer to the velocity at the top of the lower layer.

Figure 4a shows 14-bunch ray paths of the Pg phases. The ray paths covered the central part of the model between the Eastern Central Range and the Hsincheng Ridge. It is noted that better constraints existed around the transition from the active orogen to the forearc basin. The largest offset between the stations and shots was about 100 km, and the deepest ray reached down to a depth of around 10 km. On the other hand, the smallest offset of about 30 km sampled to depths of only a few kilometers, just beneath the transition zone.

Figure 4b shows a comparison of the synthetic and observed arrivals of the above Pg phases. The synthetic arrivals of most Pg phases are generally consistent with the observations. The consistence includes not only the individual travel time of each Pg phase, but also the slope of the whole group of Pg phases.

Figures 5a and 5b show 11-bunch ray paths of the PcP phases and the comparison of the observed and synthetic arrivals of those phases, respectively. As in Figure 4a, the ray paths cover the central part of the model between the Eastern Central Range and Hsincheng Ridge. There were better constraints around the transition from active orogen to forearc basin. In general, the ray coverage of the PcP phases was smaller than that for the Pg phases in the horizontal direction, but deeper than that for the Pg phases vertically. The largest offset of the recognized PcP arrivals is about 80 km, and the deepest ray was reflected from a depth of around 20 km. Based on the reflected points, all of the PcP phases can be divided into two groups. Arrivals in the first group were reflected from an east-dipping interface that is beneath the coastal line. Arrivals in the second group were reflected from a west-dipping interface beneath the Hsincheng Ridge in the oceans.

Figure 5b is a comparison of the synthetic and observed arrivals. Basically, the synthetic arrivals for most of the PcP phases fitted the observations fairly well. Again, the similarities between the synthetic and observed arrivals consist of the individual travel time of each Pg phase and the slope of the whole group of Pg phases.

Figures 6a and 6b show 12 bunches of ray paths for the PmP phases and the observed and synthetic arrivals of these phases are compared, respectively. In general, these ray paths were divided into two groups based on the reflected points. The western group, including 3 bunches

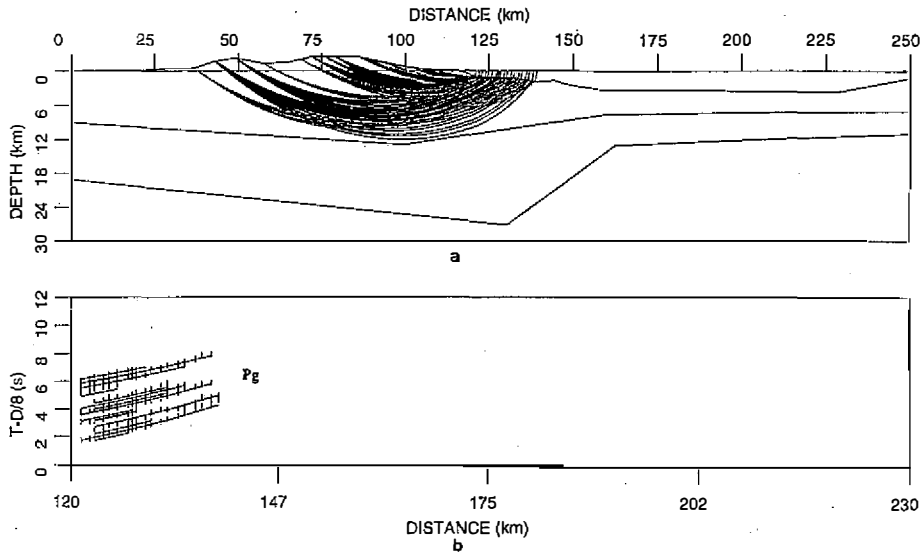

Fig. 4. Forward modeling of Pg phases. (a) Ray paths of Pg phases and (b) comparison between observed and synthetic travel time of Pg phases.

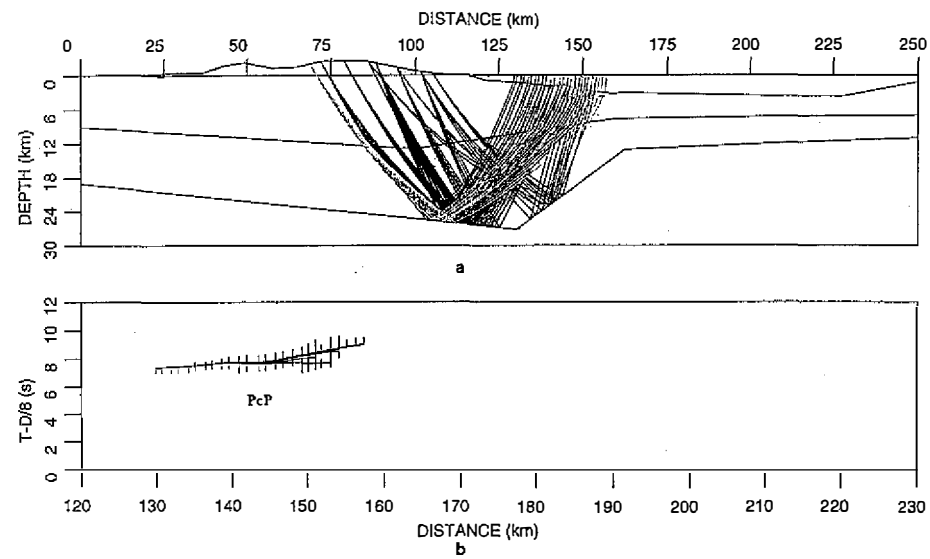

Fig. 5. Forward modeling of PcP phases. (a) Ray paths of PcP phases and (b) comparison between observed and synthetic travel time of PcP phases.

of ray paths, was the phases reflected from the Moho-discontinuity at depths greater than 40 km beneath the island of Taiwan. The eastern group, consisting of 9 bunches of ray paths, was the phases reflected from the Moho-discontinuity at depths of about 25-30 km offshore east of Taiwan. As a result, the Moho-discontinuity beneath the island is about 10 km deeper than that

in the offshore region. Although ray path constraints in the western group are significantly less than in the eastern group, both Moho-depths are quite reliable because each bunch of ray paths is composed of a number of PmP phases.

5. CRUSTAL STRUCTURES

5.1 Upper Crust

The upper crustal structures obtained from the Pg and PcP phases show the strong lateral variations across central Taiwan through the forearc basins of the westernmost part of the Ryukyu subduction system (Figure 7). In general, the velocity structures of the upper crust can be divided into two layers. The velocities within the first layer were obtained from the arrivals of the Pg phases, while those within the second layer were largely determined from the arrivals of PcP phases.

In the first layer, a wide range of velocities, from 2.9 km/sec to 5.7 km/sec was obtained. The thickness of this layer varies from 4 km to 14 km, and the deepest part is located beneath an area east of the Hualien area, near the Hsincheng Ridge. In order to see the details, we divided the areas with better constraints into three sections. The first section is at the distances between 40 km and 100 km, the second section is between 100 km and 160 km, and the third is east of 160 km from the west coast (Figure 7). For the section between 40 km and 100 km, which is beneath the Central Range, the thickness of the first layer gradually increased toward the east. It was about 12 km in depth beneath the western margin of the Central Range, and then increased to 14 km deep beneath the eastern margin of the Central Range. The velocities were about 5.0 km/sec and 5.7 km/sec at top and bottom of the layer, respectively. For the second section, around the Hsincheng Ridge, the thickness of the first layer significantly de-

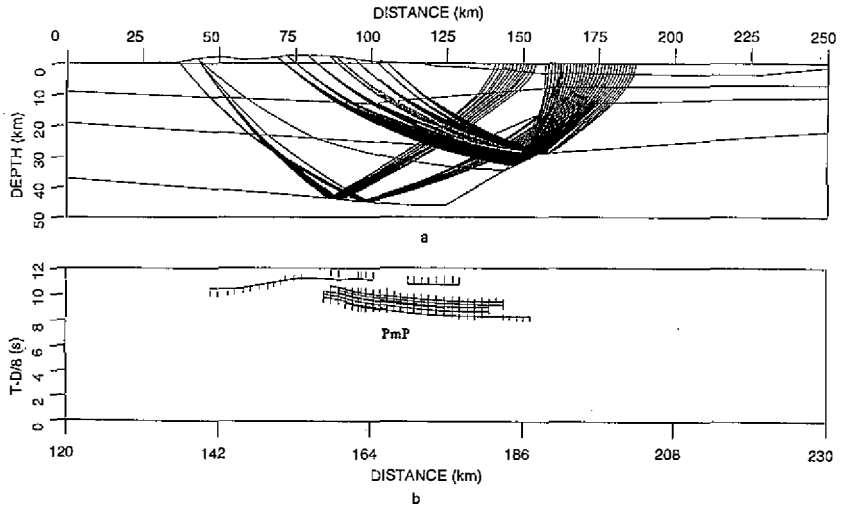

Fig. 6. Forward modeling of PmP phases. (a) Ray paths of PmP phases and (b) comparison between observed and synthetic travel time of PmP phases.

creased toward the east. It started from 14 km deep beneath the eastern margin of the Central Range to only about 4 km deep beneath the westernmost part of the Hoping Basin. The velocities in this layer significantly decreased from west to east as it extends offshore, from 5.1 km/sec to 3.9 km/sec at the top of this layer, and from 5.9 km/sec to 4.4 km/sec at the bottom. In the third section, beneath the Hoping and Nanao Basins, the thickness and velocities showed no significant variation. The thickness was around 4 km, while velocities in this layer ranged from 3.0 km/sec to 3.2 km/sec at the top, and from 5.0 km/sec to 5.5 km/sec at the bottom.

In the second layer of the upper crust, velocities of between 4.9 km/sec and 6.8 km/sec were obtained. The thickness of this layer varies from 3 km to 17 km, and the deepest part is located beneath the Hsincheng Ridge. In order to see the details, we divide the second layer into four sections. The first section is at between 50 km and 100 km from the west coast, the second section between 100 km and 125 km, the third section at between 125 km and 160 km, and the fourth section is between 160 km and 220 km from the coast. In the first section, beneath the Eastern Central Range, the thickness of the second layer dipping to the east was about 10 km. Velocities ranged from 5.6 km/sec to 5.9 km at the top of this layer and from 6.0 km/sec to 6.5 km/sec at the bottom. In the second section, beneath the Hualien area, the thickness increased eastward from 10 km to 17 km. Velocities varied from 4.9 km/sec to 6.0 km/sec at the top of this layer, and from 6.5 km/sec to 6.8 km/sec at the bottom. In the third section, just beneath the Hsincheng Ridge, the thickness of this layer significantly decreased from 17 km to only 5 km toward east. Velocities ranged from 4.9 km/sec to 6.1 km/sec at the top, and from 5.8 km/sec to 6.6 km/sec at the bottom of this layer. In the fourth section, beneath the Hoping and Nanao Basins, the thickness of this layer gradually decreased from 5 km in the west to 3 km in the east. Velocities ranged from 5.3 km/sec to 5.7 km/sec at the top, and from 5.5 km/sec to 6.0 km/sec at the bottom of this layer.

5.2 Lower Crust and Moho-Depth

Velocities obtained in the lower crust range from 6.4 - 6.7 km/sec at its top to 7.2 - 7.3 km/sec at its bottom, and the thickness of this layer varies from 12 km to 20 km (Figure 7). These results are constrained by the clear arrivals of Pc and PmP phases recorded at a number of stations. In order to see these variations in more detail, this layer is cut into three sections. From the west to the east, their ranges are defined at the horizontal distances of 70 km - 125 km, 125 km - 160 km, and 160 km - 220 km. In the first section, the depths of the lower crust gradually increase from west to east, and even the variation in its thickness is not so significant. The depths at the top and bottom of this layer are about 22 km and 41 km beneath the highest mountain on the island of Taiwan, and they increase to 28 km and 46 km, respectively, beneath the Hsincheng Ridge. In the second section, on the other hand, the lower crust shows a west-dipping layer. Although there is no visible thickness variation in the lower crust, its depth changes greatly. The depths vary from 27 km to 13 km at the top of this layer and from 44 km to 30 km at its bottom. In the third section, thickness of the lower crust decreases from 15 km to 12 km eastward. Velocities range from 5.56 km/sec to 6.29 km/sec obtained at its top, at depths of 10 ñ12 km, and increase to 7.09 ñ7.20 km/sec at its bottom, at depths of 24 ñ 30 km.

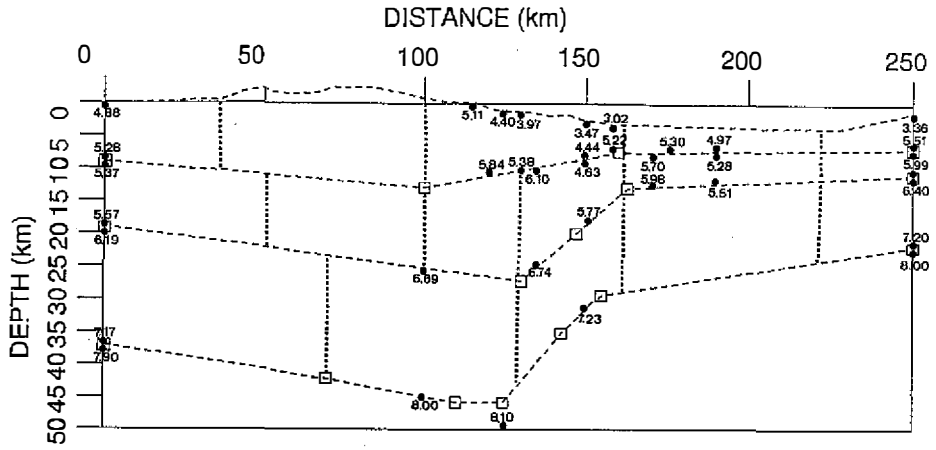

Fig. 7. Variation of Moho-depths along Taiwan Orogen and westernmost part of Ryukyu subduction system.

In Figure 7 we may also see the preliminary results of geometrical variation of the Moho-discontinuity that was directly delineated through the travel time modeling of a number of PmP phases. Generally, the Moho-discontinuity is dipping slightly (~5°) toward the east beneath the island, and steeply (~30°) toward the west beneath the Hualien and Hsincheng Ridge area. A critical point of the sharp change from east-dipping to west-dipping is found beneath just offshore beneath the Hsincheng Ridge, where the Moho-discontinuity is the deepest and about 45 km below sea level. Further east, the west-dipping trend becomes gentle beneath the Hoping and Nanao Basins. In other words, another critical corner exists at the Moho-discontinuity beneath the Hoping Basin.

6. DISCUSSIONS AND CONCLUSIONS

In general, lateral variation of velocity structures in the upper crust is stronger than that in the lower crust and uppermost mantle. Velocities at the upper crust vary from 3.0 km/sec to 6.8 km/sec. In particular, strong lateral variations of P-wave velocities obtained were directly from the slope of the Pg arrivals with a wide range of velocities between 3.0 km/sec and 5.1 km/sec in the uppermost crust. The lowest velocity was detected in the forearc basin of the Ryukyu subduction system, while the highest was in the uppermost crust in the Central Range. Those areas where velocities are less than 4.0 km/sec are largely associated with the sediments on top of ocean floor, particularly in the Hoping and Nanao basins. The results agree with these from the Multi-Channel Seismic (MCS) reflection data published by Liu (1997). On the other hand, velocities at the bottom of the upper crust of between 5.8 km/sec and 6.8 km/sec were obtained. Those velocities commonly represent the characteristics of the mid-crust, and basically confirm the results reported by Yeh and Tsai (1981), Roecker *et al.* (1987) and Lin (1996).

In addition to a wide range of velocities, strong thickness variations were obtained in the upper crust. In general, the thickness of the upper crust gradually increased from 22 km deep

beneath the western Central Range to 25 km beneath the Hsincheng ridge, with a dramatic decrease to only 10 km beneath the Hoping Basin. It is worth pointing out that the thickest part of the upper crust was located east of Hualien, beneath the Hsincheng Ridge, but not right beneath the Central Range in which the active orogeny is continuing with a strong uplifting rate (Liu, 1995). In addition, the dramatic decrease in the upper crustal thickness from 25 km to 10 km indicates a clear transition from an active orogen in Taiwan to the forearc basins of the Eurasian continental margin. The forearc basins with an upper crust thickness of about 10 km is a typical continental margin and is associated with the northward subduction of the Philippine Sea plate beneath the Eurasian plate along the westernmost Ryukyu trench.

As with the results obtained at the upper crust, strong thickness variation was found for the deep crustal structures. The crustal thickness beneath Taiwan gradually increases toward the east, and then dramatically decreases beneath the forearc basins of the westernmost part of the Ryukyu subduction system. In general, the crust thickness beneath the island could be over 40 km while being only about 25 km beneath the westernmost part of the Ryukyu forearc region. To more detail describe the variation of the Moho-discontinuity, we divide the model from west to east into three sections: (1) the Central Taiwan section, for distances less than 130 km from the west coast; (2) the Hoping Basin section, for distances between 130 km and 160 km, and (3) the Nanao Basin section, for distances greater than 160 km.

For the Central Taiwan section, the crustal thickness gradually increases toward the east with a Moho that dips slightly (about 5°). The crustal thickness is only about 35 km beneath the Western Foothills and this increases to about 45 km beneath the Eastern Central Range. This result shows that most of the crust across central Taiwan is thicker than that estimated by Yeh and Tsai (1981) and Chen (1996). The thickest crust beneath the Eastern Central Range is close to that reported by Lin (1996), who estimated that the thickest crust beneath Taiwan could be up to 45-50 km. In short, the general pattern of crustal thickness increasing toward the east is probably associated with the underthrusting of the Eurasian plate toward the east. In addition, it is worth noting that the topographic high is not well associated with the crustal thickness. There is a horizontal offset of about 40 km between the highest mountain and the thickest crust across central Taiwan. This phenomenon may indicate that Taiwan has not yet reached isostatic equilibrium, which agrees with the conclusion from gravity data (Yen *et al.*, 1995). For the Hoping Basin section, where crustal thickness dramatically decreases from 45 km to 25 km, the Moho shows a dip of about 30° toward the west. The Hoping Basin is a deformed forearc basin in the westernmost part of the Ryukyu subduction system (Liu *et al.*, 1997). The significant variation of crustal thickness in this part, within a horizontal distance of only 30 km, indicates a sharp transition from an active orogen in central Taiwan to the westernmost part of the Ryukyu subduction system. For the section east of the Hoping Basin, the crust thickness decreases slightly toward the east from 25 km to 20 km. Such a result might suggest a typical crustal thickness for the Eurasian continental margin.

Acknowledgments The authors would like to thank the many colleagues and students from the Institute of Earth Sciences, Academia Sinica, National Chung Cheng University, National Taiwan University and National Central University, who gave their great support during field work. Also appreciated is the IRIS for providing parts of the Reftek instruments and the crew of the R/V Ewing for providing powerful air-gun shots. In addition, we thank Dr. CharShine

Liu for providing much of the valuable information and comments, and Dr. C. Zelt for providing the modeling program. We also thank the reviewers for their valuable comments. This work was generously supported by the National Science Council of the Republic of China, under grant NSC85-2111-M-001-011Y, NSC86-2116-M-194-003Y, NSC85-2111-M-001-011 and NSC85-2116-M-001-019-Y.

REFERENCES

Angelier, J., and E. Barrier, 1986: Active collision in eastern Taiwan: The Coastal Range. *Mem. Geol. Soc. China*, **7**, 135-159.

Biq, C., 1972: Dual-trench structure in the Taiwan-Luzon region. *Proc. Geol. Soc. China*, **15**, 67-75.

Bowin, C., R. S. Lu, C. S. Lee, and H. Schouten, 1978: Plate convergence and accretion in the Taiwan-Luzon region. *Am. Assoc. Petrol. Geol. Bull.*, **62**, 1645-1672.

Chen, C. H., 1996: Moho-depths determined from gravity spectrum in the Taiwan area, Master's Thesis, National Chung-Cheng University, 62 pp.

Ho, C. S., 1982: Tectonic evolution of Taiwan: Explanatory text of the tectonic map of Taiwan: Taipei, ROC, Ministry of Economic Affairs, Taipei, 126 pp.

Lin, C. H., 1996: Crustal structures estimated from arrival differences of the first P-waves in Taiwan. *J. Geol. Soc. China*, **39**, 1-12.

Liu, C. S., P. Schnurle, S. Lallemand, and D. L. Reed, 1997: TAICRUST and deep seismic imaging of western end of the Ryukyu Arc-Trench system, JAMSTEC J. of Deep Sea Research, special volume: Deep sea research in subduction zones, spreading centers and backarc basins. 39-45.

Pelletier, B., and J. F. Stephan, 1986: Middle Miocene obduction and late Miocene beginning of collision registered in the Hengchun Peninsula: Geodynamic implications for the evolution of Taiwan. *Mem. Geol. Soc. China*, **7**, 301-324.

Rau, R. J., and F. T. Wu, 1995: Tomographic imaging of lithospheric structures under Taiwan. *Earth Planetary Sci. Lett.*, **133**, 517-532.

Roecker, S. W., Y. H. Yeh, and Y. B. Tsai, 1987: Three-dimensional P and S wave velocity structures beneath Taiwan: Deep structure beneath an arc-continent collision. *J. Geophys. Res.*, **92**, 10547-10570.

Tsai, Y. B., 1978: Plate subduction and the Plio-Pleistocene orogeny in Taiwan. *Petrol. Geol. Taiwan*, **15**, 1-10.

Yeh, Y. H., and Y. B. Tsai, 1981: Crustal structures of central Taiwan from inversion of P-wave arrival times. *Bull. Inst. Earth Sciences*, **1**, 83-102.

Yeh, Y. H., R. C. Shih, C. H. Lin, C. C. Liu, H. Y. Yen, B. S. Huang, C. S. Liu, P. Z. Chen, C. S. Huang, C. J. Wu, and F. T. Wu, 1998: Onshore/offshore wide-angle seismic profiling in Taiwan. *TAO*, **9**, 301-316.

Yen, H. Y., Y. H. Yeh, C. H. Lin, K. J. Chen, and Y. B. Tsai, 1995: Gravity survey of Taiwan. *J. Physical Earth*, **43**, 683-696.

Zelt, C. A., and R. B. Smith, 1992: Seismic traveltime inversion for 2-D crustal velocity structure. *Geophys. J. Int.*, **108**, 16-34.